AGU ADVANCING EARTH AND SPACE SCIENCES

Geophysical Research Letters®

RESEARCH LETTER
10.1029/2023GL104155

Influences of East Asian Winter Monsoon and El Niño-Southern Oscillation Variability on the Kuroshio Intrusion to the South China Sea Over the Past 60 Years

Ke Lin[1,2], Tao Han[3], Yilin Zhang[2], Chuan-Chou Shen[1,4], Shih-Yu Lee[5], Jingyu Wang[6], Ahmad T. Mohtar[2], Kuo-Fang Huang[7], Hong-Wei Chiang[5], Yue-Gau Chen[1,5], and Xianfeng Wang[2]

[1]Department of Geosciences, National Taiwan University, Taipei, Taiwan, [2]Earth Observatory of Singapore, Asian School of the Environment, Nanyang Technological University, Singapore, Singapore, [3]State Key Laboratory of Loess and Quaternary Geology, Institute of Earth Environment, Chinese Academy of Sciences, Xi'an, China, [4]Research Center for Future Earth, National Taiwan University, Taipei, Taiwan, [5]Research Center for Environmental Changes, Academia Sinica, Taipei, Taiwan, [6]National Institute of Education, Nanyang Technological University, Singapore, Singapore, [7]Institute of Earth Sciences, Academia Sinica, Taipei, Taiwan

Abstract The Kuroshio intrusion (KI) is a northwestward-flowing branch of the Kuroshio Current, which enters the South China Sea (SCS) and regulates its temperature, salinity, and water mass exchanges. However, limited direct observations hinder our understanding of KI's mechanisms and responses to climate change. Here, we present a 60-year bi-monthly resolved coral oxygen isotope (δ^{18}Oc) record from Dongsha Atoll, the northern SCS. The dry-season (December–March) δ^{18}Oc record reveals interannual to decadal variabilities of the KI. The impact of the East Asian winter monsoon (EAWM) on Dongsha δ^{18}Oc was more pronounced during the 1970s and 1980s and after the early 2000s, while the influence of the El Niño-Southern Oscillation (ENSO) on Dongsha δ^{18}Oc was higher between the 1980s and 1990s. The Pacific Decadal Oscillation (PDO) may have a relatively minor effect on KI strength or may indirectly modulate KI strength through its influence on ENSO activities. Our Dongsha δ^{18}Oc record highlight the importance of the EAWM, ENSO, and PDO in predicting future KI changes.

Plain Language Summary The Kuroshio intrusion is a branch of the Kuroshio Current. It flows into the South China Sea and affects its temperature, salinity, and water movement. We however know very little how the Kuroshio intrusion responds to climate changes. Here we present a study on the chemical composition of a coral core from Dongsha Atoll in the northern South China Sea. Our study shows that the intrusion varies markedly over the past 60 years and is connected to changes in sea surface salinity. Stronger intrusions align with stronger East Asian winter monsoon intensity and El Niño events. Understanding how the Kuroshio intrusion reacts to climate change is important for effectively managing the potential impacts of global warming on the marine ecosystem.

Key Points:

- A 60-year-long coral oxygen isotope record from Dongsha Atoll, South China Sea reveals interannual to decadal variations in the Kuroshio intrusion
- Strong Kuroshio intrusion, corresponding to high sea surface salinity, is identifiable over the past 60 years
- The Kuroshio intrusion variations are primarily driven by East Asian winter monsoon changes and also influenced by El Niño-Southern Oscillation

Supporting Information:

Supporting Information may be found in the online version of this article.

Correspondence to:

K. Lin and Y.-G. Chen,
linke@ntu.edu.sg;
ygchen@gate.sinica.edu.tw

Citation:

Lin, K., Han, T., Zhang, Y., Shen, C.-C., Lee, S.-Y., Wang, J., et al. (2024). Influences of East Asian winter monsoon and El Niño-Southern Oscillation variability on the Kuroshio intrusion to the South China Sea over the past 60 years. *Geophysical Research Letters*, *51*, e2023GL104155. https://doi.org/10.1029/2023GL104155

Received 16 APR 2023
Accepted 18 DEC 2023

Author Contributions:

Conceptualization: Ke Lin
Formal analysis: Ke Lin
Investigation: Tao Han
Methodology: Ke Lin, Tao Han, Yilin Zhang, Shih-Yu Lee, Ahmad T. Mohtar
Resources: Hong-Wei Chiang
Supervision: Yue-Gau Chen, Xianfeng Wang
Validation: Chuan-Chou Shen

1. Introduction

The Kuroshio Current is a warm western boundary current that originates from the Western Equatorial Pacific and flows northeastward to the North Pacific. After passing by the east coast of the Philippines, the Kuroshio Current branches northwestward into the South China Sea (SCS) through the Luzon Strait, and creates what is known as the Kuroshio intrusion (KI). The KI is characterized by relatively warmer and higher salinity waters and can cause significant impacts on the hydrological conditions in the SCS (e.g., Chang et al., 2022; Hu et al., 2000; Liang et al., 2008; Nan et al., 2015; Qu et al., 2004). Moreover, the KI brings nutrient-rich water, creating favorable conditions for planktonic organisms and facilitating biodiversity in the SCS (e.g., Chen, 2008; Chou et al., 2007; T. Li et al., 2010). Changes in the KI can then modulate not only the hydrological conditions (e.g., heat and salt budgets, and circulation) but also the marine ecosystem (e.g., trophic interactions, species dynamics, and biogeochemical processes) in the SCS. In recent decades, increasing efforts have been garnered to understand the behavior and variability of the KI. Instrumental data from hydrographic surveys, moored buoys, and remote sensing, have been used to monitor the physical properties of the water and track the movement of the KI (e.g., Centurioni et al., 2004; Liu et al., 2016; Shaw, 1991). Paleodata, such as records from corals and sediment cores, have also been employed to assess the long-term

Writing – original draft: Ke Lin
Writing – review & editing: Chuan-Chou Shen, Jingyu Wang, Kuo-Fang Huang, Yue-Gau Chen, Xianfeng Wang

variability of the KI (e.g., Chang et al., 2022; X. Li et al., 2017, 2023; Ramos et al., 2020; Shen et al., 2022). However, these studies have their limitations. For example, instrumental observations only cover the past few decades, so they may not be long enough to capture the long-term variability of the KI. On the other hand, the few available paleoclimate studies, mostly coral records from the north of the Luzon Strait (e.g., X. Li et al., 2017, 2023; Ramos et al., 2020), substantially extend the KI history by using geochemical proxies, such as monthly resolved coral $\delta^{18}O$. However, the strong turbulence and shallow topography near their study sites, may limit the reconstruction of KI strength (Figure 1) because of the contribution of subsurface cold water resulted from tidally induced upwelling (Lee et al., 1997; C.-C. Shen et al., 2005). Additionally, because the KI is typically much stronger in winter (December–March) than in summer (June–September), the KI characterization can be underestimated if seasonal signals are not separated in the studies, as suggested by Ramos et al. (2020).

The mechanisms that control the KI have also been explored, which involve the East Asian winter monsoon (EAWM), El Niño-Southern Oscillation (ENSO), and Pacific Decadal Oscillation (PDO) (Y. Y. Kim et al., 2004; Qu et al., 2004; Ramos et al., 2020; Rong et al., 2007; Y. Wang et al., 2020; C.-R. Wu, 2013; Yuan et al., 2014). On the interannual timescale, the strength of the KI into the SCS is enhanced (suppressed) when the EAWM is anomalously strong (weak) (C. Wu & Hsin, 2012; Xue et al., 2004). However, this relationship can be complicated by ENSO. El Niño conditions are typically accompanied by a weakened EAWM (B. Wang et al., 2000), but they also enhance KI strength in winter (Yuan et al., 2014). Moreover, statistical analysis shows that KI strength has increased during the positive PDO phase since 1991 (C.-R. Wu, 2013). However, a reconstruction of dry season (December–March) sea surface salinity (SSS) using paired *Porites* Sr/Ca and $\delta^{18}O$ from southern Taiwan suggests a strong negative correlation between the SSS variability across the Luzon Strait and the PDO, particularly at multidecadal timescales (Ramos et al., 2020). Apparently, the interactions among the three climate modes (EAWM, ENSO, and PDO) can complicate the responding changes in KI strength and SSS in the region.

In this study, we present a bimonthly resolved record of coral $\delta^{18}O$ and Sr/Ca from a living *Porites* coral core obtained from Dongsha Atoll, which covers a time period from 1952 to 2016. The coral site is located in the northern part of the SCS, an area frequently influenced by the KI through the Luzon Strait (Figure 1). Therefore, changes in the KI, which affect the local sea surface temperature (SST) and SSS, may be reconstructed by the chemical composition of coral skeletons. Our study has two main objectives: First, to investigate the potential of using Dongsha coral Sr/Ca and $\delta^{18}O$ variations to infer KI variability. This will be done by comparing the coral Sr/Ca and $\delta^{18}O$ records in the cold/dry season (December–March) with KI strength, indicated here by the sea surface height (SSH) difference between the eastern side of the Luzon Strait and the adjacent SCS. The strait serves as a narrow passage connecting the western Pacific Ocean to the SCS. Prevailing winds and ocean currents lead to higher SSH on the eastern side, creating a pressure gradient propelling the KI into the SCS. KI strength can be assessed by the SSH difference between the two sides of the strait; elevated SSH in the east intensifies KI flow into the SCS (Figure 1). Hence, variations in the SSH gradient play a crucial role in regulating KI strength and variability in the SCS (e.g., Caruso et al., 2006; Nan et al., 2011, 2013; F.-H. Xu & Oey, 2015). And second, to explore the hydrological changes associated with KI variability on interannual to decadal timescales within the region, and the possible impacts of large-scale climatic modes such as EAWM, ENSO, and PDO on the KI variability in the SCS.

2. Materials and Methods

2.1. Study Site

The northern SCS (delineated here as the region north of 18°N) is unique due to monsoon winds and water exchange with the western tropical Pacific via the Luzon Strait (Shu et al., 2018; F.-H. Xu & Oey, 2015). Dongsha Atoll, located at 20.58–20.78°N, 116.68–116.92°E, is the northernmost atoll in the SCS and has a diameter of 28 km (Figure 1). The climate is subtropical and influenced by the East Asian Monsoon. The warm and wet months occur from June to September (JJAS), while the cold and dry months last from December to March (DJFM) (Figure S1 in Supporting Information S1). Annual rainfall is approximately 1,100 mm, and annual SSS ranges from 33.8 to 34.5 psu (practical salinity unit) with a mean amplitude of 0.4 psu. The annual average temperature is 26.4°C during the period from 1982 to 2016, with the highest monthly averaged temperature in July (29.2°C) and the lowest monthly temperature in February (23.0°C).

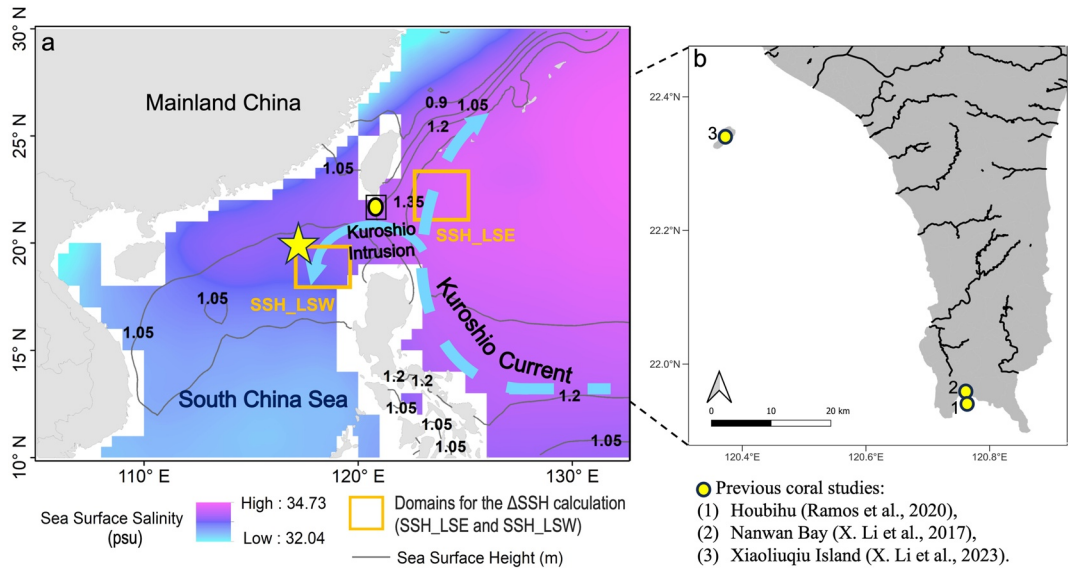

Figure 1. (a) Map of sea surface salinity (SSS) and sea surface height (SSH) in the Northern South China Sea (SCS) with Kuroshio Current (blue dashed arrow) and a westward branch of the Kuroshio Current, also known as the Kuroshio intrusion (KI) (blue arrow). The yellow star indicates the Dongsha Atoll, where a coral core DS86 was collected. The blue circle shows the locations of the three published coral proxy records from the north of the Luzon Strait (i.e., X. Li et al., 2017, 2023; Ramos et al., 2020). For our analysis, we utilized IAP-05 SSS data at a depth of 10 m spanning from 1993 to 2018. The SSH data for the period 1993–2019 was obtained from the AVISO website (http://www.aviso.altimetry.fr/en/home.html) and processed into a grid format with a spatial resolution of 1° by 1°. The red rectangles mark the selected locations for ΔSSH calculation. SSH_LSE and SSH_LSW refer to the sea surface heights in the regions located in the eastern and western sides of the Luzon Strait, respectively. (b) Also shown are sites of previous coral studies in southern Taiwan, including (1) Houbihu (Ramos et al., 2020), (2) Nanwan Bay (X. Li et al., 2017), and (3) Xiaoliuqiu Island (X. Li et al., 2023).

2.2. Coral Sampling and Analytical Methods

In August 2016, a 50 cm long and 8 cm diameter coral core (DS86) was collected from a *Porites* coral colony at Dongsha Atoll (20.62°N, 116.7°E, Figure 1). The core was cut into 7 mm-thick slabs, X-rayed for annual density bands (Figure S2a in Supporting Information S1), and assessed for mineral diagenesis (Text S1 and Figure S2b in Supporting Information S1). Sub-samples for $\delta^{18}O$ and Sr/Ca measurements were collected every millimeter along the maximum growth axes identified in the X-ray radiographs (Text S2 and Figure S2a in Supporting Information S1). Coral $\delta^{18}O$ ($\delta^{18}Oc$) was measured using an isotope ratio mass spectrometer (IRMS, Thermo Scientific Delta V) coupled to GasBench II, and Sr/Ca was measured using a high-resolution inductively coupled plasma mass spectrometer (HR-ICP-MS, Thermo Fisher Scientific ELEMENT 2) (Text S3 in Supporting Information S1). All the sample preparations and analyses for stable isotopes and trace elements were conducted at the Earth Observatory of Singapore, Nanyang Technological University. The coral skeleton grows at an average rate of approximately 7 ± 1.7 mm per year, enabling us to generate approximately 7 subsamples annually (Text S4 and Figure S3 in Supporting Information S1). Subsequently, the coral $\delta^{18}O$ and Sr/Ca data were interpolated to create bi-monthly time series with six data points per year (Text S4 and Figure S4 in Supporting Information S1).

2.3. Satellite and In Situ Data to Retrieve SST and SSS

In this study, SST, SSS, and rainfall records obtained from existing instrumental data sets were used to calibrate the reconstructed variables. To calibrate reconstructed SST, we extracted NOAA OISST data from 1981 to 2016 in a 1/4° by 1/4° grid centered at 20.5°N and 116.5°E (https://www.ncei.noaa.gov/products/climate-data-records/sea-surface-temperature-optimum-interpolation, Huang et al., 2021). For calibration of reconstructed SSS, we used the monthly mean SSS data from the Institute of Atmospheric Physics global ocean salinity 0.5° gridded data set (IAP-05) centered at 20.5°N and 116.5°E from 1960 to 2020 (http://www.ocean.iap.ac.cn/pages/dataService/dataService.html?languageType=en&navAnchor=dataService, G. Li et al., 2023). For rainfall comparison with Dongsha $\delta^{18}Oc$ data, we used a larger spatial data set (2.5° × 2.5° averaged, 20–22.5°N; 115–117.5°E,

1979–2020) from NASA's Global Precipitation Climatology Project (GPCP) (http://disc2.nascom.nasa.gov/Giovanni/tovas/rain.GPCP.shtml, Adler et al., 2003).

2.4. The Sea Surface Height (SSH) Calculation

Satellite altimeter data from the Luzon Strait has frequently served as an indicator of the KI's intensity into the SCS (e.g., Nan et al., 2011, 2013). To assess the strength of the KI into the SCS, we calculated the monthly difference in SSH between the eastern side of the Luzon Strait and the adjacent SCS. Daily altimetry satellite data spanning from 1993 to 2016, with a spatial resolution of 1° by 1°, were acquired from the AVISO website (http://www.aviso.altimetry.fr/en/home.html) for this calculation. This difference, denoted as ΔSSH, was obtained by subtracting the monthly average SSH in the SCS region from the monthly average SSH on the eastern side of the Luzon Strait (Figure 1, Text S5 in Supporting Information S1).

2.5. Spectral Analysis

To conduct spectral analysis on the coral $\delta^{18}O$ data, we applied the Multitaper Method (MTM) using the SSA-MTM Toolkit, following the parameters set by Ghil et al. (2002), which included a resolution setting of 2 and the use of 3 tapers. Before subjecting the data to spectral analysis, a linear detrending process was implemented to ensure the accuracy of the results. To establish confidence levels, we adopted a red noise AR(1) background. We performed wavelet and cross-wavelet analyses using the wavelet coherence methods initially developed by Grinsted et al. (2004). To assess significance, we conducted 300 Monte Carlo simulations and evaluated the 95% confidence level against the red noise background.

3. Results

3.1. Bi-Monthly Calibration of Sr/Ca to SST

The Sr/Ca values of DS86 range from 8.738 to 9.262 mmol/mol, with an average of 8.971 mmol/mol (Figure 2a; Figure S4 in Supporting Information S1). We first conducted a spatial correlation analysis between Dongsha coral Sr/Ca and NOAA OISST data (Figure S5 in Supporting Information S1), confirming that Dongsha coral Sr/Ca can capture SST variabilities in the northern SCS. To ensure the robustness of the SST-proxy relationships at bi-monthly scales, we then performed an evaluation using the Reduced Major Axis (RMA) regression method. This approach helps mitigate any biased estimates of SST (DeLong et al., 2007; C. Xu et al., 2015). The results are expressed in Equation 1 and Figure S6 of the Supporting Information S1:

$$\mathrm{Sr/Ca\,(bi\text{-}monthly)} = 10.338(\pm 0.033) - 0.053(\pm 0.001) \times \mathrm{OISST\,(^{\circ}C)}.$$

$$(r = -0.93, p \ll 0.001, n = 207, \mathrm{RMSR} = 0.809^{\circ}\mathrm{C}, 1982 - 2016).$$

where RMSR (°C) is the root mean square of the residuals that indicates the difference between the instrumental and reconstructed SSTs. The Sr/Ca-SST regression of coral DS86 yielded a slope of −0.053 mmol/mol per °C, within the range of slope values reported in *Porites*-based Sr/Ca-SST studies (i.e., −0.042 to −0.067 mmol/mol per °C, RMA regression method; e.g., Murty et al., 2018; Quinn & Sampson, 2002; Ramos et al., 2020).

3.2. δ^{18}Oc-SST/SSS Relationships

3.2.1. Relationship Between δ^{18}Oc and SST at Bi-Monthly Scales

The δ^{18}Oc values of DS86 average −4.54‰ and vary from −5.61‰ to −3.13‰. The δ^{18}Oc shows clear annual cycles reflecting winter and summer seasons (Figure 2b). We first compared the δ^{18}Oc and Sr/Ca profiles in Dongsha coral (Figure S4 in Supporting Information S1). Their strong correlation at the bi-monthly scale ($r = 0.72$, $p < 0.001$, $n = 387$, Figure S7 in Supporting Information S1), suggests that the two variables share common control factors, primarily SST. We then compared δ^{18}Oc variability with instrumental SST (Figure S8 in Supporting Information S1). The RMA regression revealed that δ^{18}Oc indeed has a moderate, but statistically significant correlation with instrumental SST ($r = -0.63$, $p < 0.001$, Equation 2), suggesting that other factors besides SST may also influence δ^{18}Oc variations.

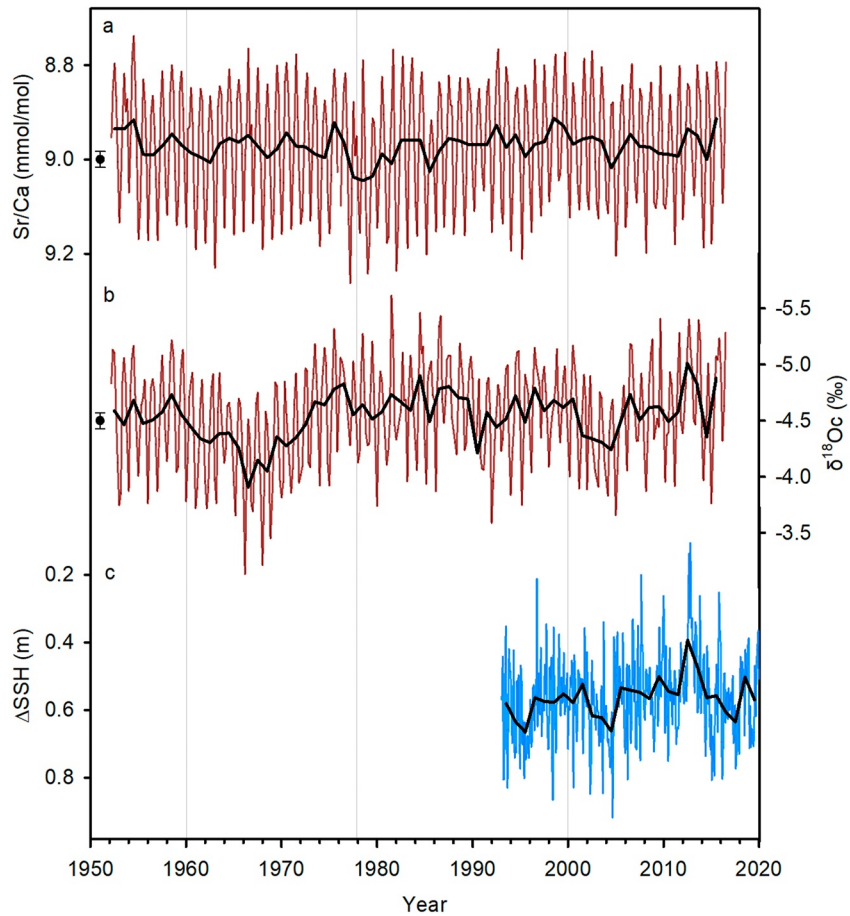

Figure 2. Bi-monthly time series data for Dongsha coral DS86, including (a) Sr/Ca and (b) δ^{18}Oc measurements from 1952 to 2016, as well as (c) the ΔSSH record from 1993 to 2019. The error bars on the left side of the coral records indicate analytical precision (1σ). A higher ΔSSH value indicates a stronger KI, while a lower value suggests a weaker intrusion. Each record is represented by an annual mean, denoted by a bold black line.

$$\delta^{18}\mathrm{O\,(bi\text{-}monthly)} = 0.170(\pm 0.241) - 0.183(\pm 0.010) \times \mathrm{OISST\,^{\circ}C}.$$

$$(r = -0.63, p < 0.001, n = 207, \mathrm{RMSR} = 1.725^{\circ}\mathrm{C}, 1982 - 2016).$$

The linear regression between coral δ^{18}Oc and instrumental SST resulted in a slope of −0.183‰/°C, similar to previously published values for corals in the SCS (i.e., −1.142–0.174‰/°C) (Bolton et al., 2014; He et al., 2002; Shen et al., 1996, 2005; Su et al., 2006; Yu et al., 2005). However, the precision of δ^{18}Oc-SST reconstructions is lower than that of Sr/Ca-SST (Figure S8 in Supporting Information S1). The δ^{18}Oc-SST RMSR of 1.725°C was considerably higher than the Sr/Ca-SST RMSR of 0.809°C, indicating reduced accuracy in predicting SST from δ^{18}Oc. Together with the modest correlation between the δ^{18}Oc and SST, it suggests that other factors, such as SSS of surrounding seawater, can also have important influence on δ^{18}Oc variations (Dassié et al., 2014; Gagan et al., 1994; Linsley et al., 2004; Lough, 2010; McConnaughey, 1989).

3.2.2. Interannual Relationships of δ^{18}Oc to SST and SSS

We calculated the relative contributions of SST and SSS to δ^{18}Oc (Text S6 in Supporting Information S1). We found that SSS accounts for approximately 32%–46% of the δ^{18}Oc signals during the dry season (December–March) and on annual timescale when comparing with NOAA OISST and IAP-05 SSS for the period of 1982–2015. These results indicate that the contribution of SSS cannot be ignored. Because of the significant correlation between Sr/Ca and OISST at bi-monthly timescale, the SSS component in δ^{18}Oc (i.e., δ^{18}Osw) may be isolated by removing the Sr/Ca-based SST component from the δ^{18}Oc signals. Text S7 in Supporting

Information S1 indicates the resultant δ^{18}Osw and its correlation with SSS. However, the relationship between δ^{18}Osw and IAP-05 SSS in coral DS86 exhibit a weak correlation (Figure S9 in Supporting Information S1). The error in reconstructed SSS from the δ^{18}Osw-SSS calibration also exhibits larger variability compared to the reconstructed SSS from the δ^{18}Oc-SSS calibration.

One possible explanation for this observation is that during the dry season (December–March), Dongsha Atoll experiences a combination of cold (low SST) and dry (high SSS) conditions. However, the KI is strong during the dry season (December–March) and brings relatively warm (high SST) and salty (high SSS) water to the region. Consequently, intense Kuroshio intrusion results in competing temperature effects and complicates the quantification of the SST contribution in δ^{18}Oc. On the other hand, when comparing bimonthly δ^{18}Oc variability with IAP-05 SSS, we found a moderate correlation ($r = 0.52$, $p < 0.001$, $n = 207$, 1982–2016, Figure S10 in Supporting Information S1). Therefore, a reasonable approach is to utilize δ^{18}Oc variability to investigate KI behavior, which considers both temperature and salinity aspects. We then examined the δ^{18}Oc variation during the dry season (December–March), with a focus on the stronger influence of the KI in winter.

We also performed spectral analysis on the bi-monthly δ^{18}Oc record during the dry season (December–March). We averaged the bimonthly record from December to March to create a dry-season interannual record. The analysis revealed highly significant periods at 2.1, 2.9, and 3.2 years, as well as a prominent ~33-year peak (Figure S11 in Supporting Information S1). These periods exhibited significance levels exceeding 95% and 90%, respectively, indicating the presence of interannual to decadal changes in the δ^{18}Oc record. This allows us to further investigate how the KI responds to the impacts of various climate modes across distinct time scales.

3.2.3. Interannual Relationships of δ^{18}Oc to Rainfall

Previous studies suggested that salinity signals in the SCS and surrounding regions can be influenced by the monsoon system and its associated precipitation (Durack et al., 2012; Liu et al., 2018; SChmitt, 2008; Shen et al., 2005; Su et al., 2006; Terray et al., 2012; Yu et al., 2005). To investigate the relationship between SSS and precipitation in Dongsha Atoll of the SCS, we analyzed the correlation between IAP-05 SSS and GPCP precipitation data from 1979 to 2016. Our findings show a moderate negative correlation between monthly IAP-05 SSS and GPCP precipitation ($r = -0.48$, $p < 0.001$, $n = 455$), suggesting that precipitation is only one of the factors affecting SSS signals in the SCS. We further analyzed the relationship between these variables during the dry season (December–March), when the KI occurs. The correlation between IPA-05 SSS and GPCP precipitation is particularly weak during the dry season (December–March) ($r = -0.15$, $p < 0.001$, $n = 147$), implying that precipitation only has a trivial contribution to SSS variations during this season.

Additionally, to explore the relationship between precipitation and the δ^{18}O signal in the coral, we conducted RMA regressions on the bi-monthly δ^{18}Oc values and GPCP precipitation. The analysis revealed a weak negative correlation between δ^{18}Oc and GPCP precipitation ($r = -0.30$, $p = 0.004$, $n = 225$, 1979–2016). However, we observed no correlation between δ^{18}Oc and GPCP precipitation during the dry season (December–March) ($r = -0.02$, $p < 0.001$, $n = 75$, 1979–2016), suggesting that other climatic factors play a dominant role in shaping δ^{18}Oc variability during this season.

3.3. The ΔSSH Record and Other KI Index

To evaluate our ΔSSH as a proxy for KI strength, we compared the ΔSSH record with a previously defined index to measure the KI into the SCS (hereby, KIS) by C.-R. Wu et al. (2017). Note that, our ΔSSH reflects the variability in SSH across the Luzon Strait, which essentially drives the KI. In contrast, the KIS index from C.-R. Wu et al. (2017) only quantified the monthly mean sea level within a spatial subdomain of the SCS (115–120°E, 15–20°N), which might be influenced by local wind patterns as well as potential height variations. Despite the differences in their definitions, Figure S12 in Supporting Information S1 shows that both indices display a similar pattern and variability. The correlation is noteworthy, with a coefficient of $r = -0.83$ ($p < 0.05$, $n = 22$) when applying a 3-year average and $r = -0.88$ ($p < 0.01$, $n = 24$) when using an 11-year low-pass filter.

Additionally, we conducted a comparison between the calculated ΔSSH record and our δ^{18}Oc during the dry season (December–March) and the wet season (June–September) from 1993 to 2015 to examine the relationship between the KI and δ^{18}Oc variations in different seasons. Figure S13 in Supporting Information S1 illustrates a robust correlation between the ΔSSH record and our δ^{18}Oc record, particularly during the dry season

(December–March) ($r = 0.92$, $p < 0.05$, $n = 23$), when applying an 11-year low-pass filter. This finding supports the robustness of our δ^{18}Oc record in capturing KI signals on decadal timescales.

4. Discussion

4.1. Coral-Derived Sr/Ca and δ^{18}Oc in the Northern SCS

Coral-inferred SST and SSS records have been used to investigate hydrological patterns in the tropical Pacific and the SCS (e.g., Bolton et al., 2014; Nurhati et al., 2011; Ramos et al., 2020). We observed a strong correlation between our coral-derived proxies (Sr/Ca and δ^{18}Oc) and instrumental data (i.e., OISST and IAP-05 SSS). However, it is important to validate the sensitivity of coral Sr/Ca and δ^{18}O to regional environmental and climatic changes, as these may differ between coral colonies (Alpert et al., 2016; Correge et al., 2004; Sayani et al., 2019), due to vital effects (Kuffner et al., 2012; Watanabe et al., 2007) or stressful conditions (Marshall & McCulloch, 2002).

To address these issues, we compared our coral Sr/Ca and δ^{18}O records with those from Houbihu, southern Taiwan (Ramos et al., 2020). We observed a similar pattern of Sr/Ca profiles between Dongsha and Houbihu during their contemporaneous growth period of 1952–2012 ($r = 0.74$, $p < 0.01$, Figure S14 in Supporting Information S1). Furthermore, the average Sr/Ca value in Dongsha of 8.97 mmol/mol is slightly higher than that of Houbihu (1952–2012) at 8.89 mmol/mol. This observation is consistent with instrumental data that shows SST is generally lower in Dongsha Atoll than that of Houbihu. Our Dongsha record also exhibits a similar trend in δ^{18}Oc compared to other coral records from southern Taiwan (e.g., X. Li et al., 2017, 2023; Ramos et al., 2020) at both bi-monthly and annual timescales (Figure S15 in Supporting Information S1). This similarity suggests that our Dongsha record reliably captures the variations in SSS/SST within the northern SCS region.

4.2. Reconstruction of the KI From Dongsha Coral Geochemistry Proxies

A stronger KI is expected to increase the influx of warm and salty water into the SCS during the dry season (December–March), resulting in higher SST and SSS. Previous studies have explored the relationship between the KI transport and SST in the northern SCS. For example, Farris and Wimbush (1996) suggested that SST may not be a reliable indicator to distinguish the KI pathway from the SCS waters when the temperature difference between the KI and the SCS surface water is smaller in summer. However, Chang et al. (2022) suggested that SST can be used to investigate the long-term KI changes because intense KI will cause more cold subsurface water of Kuroshio Current to upwell onto the surface, resulting in cooler SST, and vice versa. Additionally, the temperature-salinity dominated coral geochemical signals from southern Taiwan were used as proxies to investigate changes in the Kuroshio Current and KI transports (e.g., X. Li et al., 2017, 2023; Ramos et al., 2020). To investigate the relationship between the strength of the KI into the SCS and coral-derived Sr/Ca record, we compared Dongsha coral Sr/Ca record with the ΔSSH record during the dry season (December–March). Figure S16 in Supporting Information S1 shows that the Sr/Ca record does not exhibit a significant relationship with the strength of the KI into the SCS, implying that SST reconstructed from Dongsha coral cannot differentiate KI water from SCS water. As the strong KI in the Luzon Strait occurs in the dry season (December–March) when the SCS water becomes colder, the temperature difference between the KI and the SCS surface water may not be indiscernible to observe in coral-inferred SST records. Taken together, Dongsha Sr/Ca record mainly reflects regional SST variations rather than the KI transport.

In contrast, Dongsha δ^{18}Oc and the ΔSSH records during the dry season (December–March) exhibit a similar pattern between 1993 and 2015 (Figures S13 and S16 in Supporting Information S1). The relationship between the two records become even stronger when applying a 3-year average and an 11-year low-pass filter (Figure S17 in Supporting Information S1). Thus, Dongsha δ^{18}Oc can serve as a sensitive and reliable proxy for KI variability. This agreement also suggests that water mass advection from the Luzon Strait, which is primarily influenced by KI strength, has a significant impact on the SSS variability of the surrounding waters at Dongsha Atoll.

Dongsha δ^{18}Oc record presents clear interannual and decadal variations. In particular, the record registers relatively high δ^{18}Oc between the early 1950s and the late 1960s, with the maximum δ^{18}Oc appeared in the mid 1960s. This indicates that KI strength also varies on interannual and decadal timescales, and likely reached its strongest condition during the mid to late 1960s.

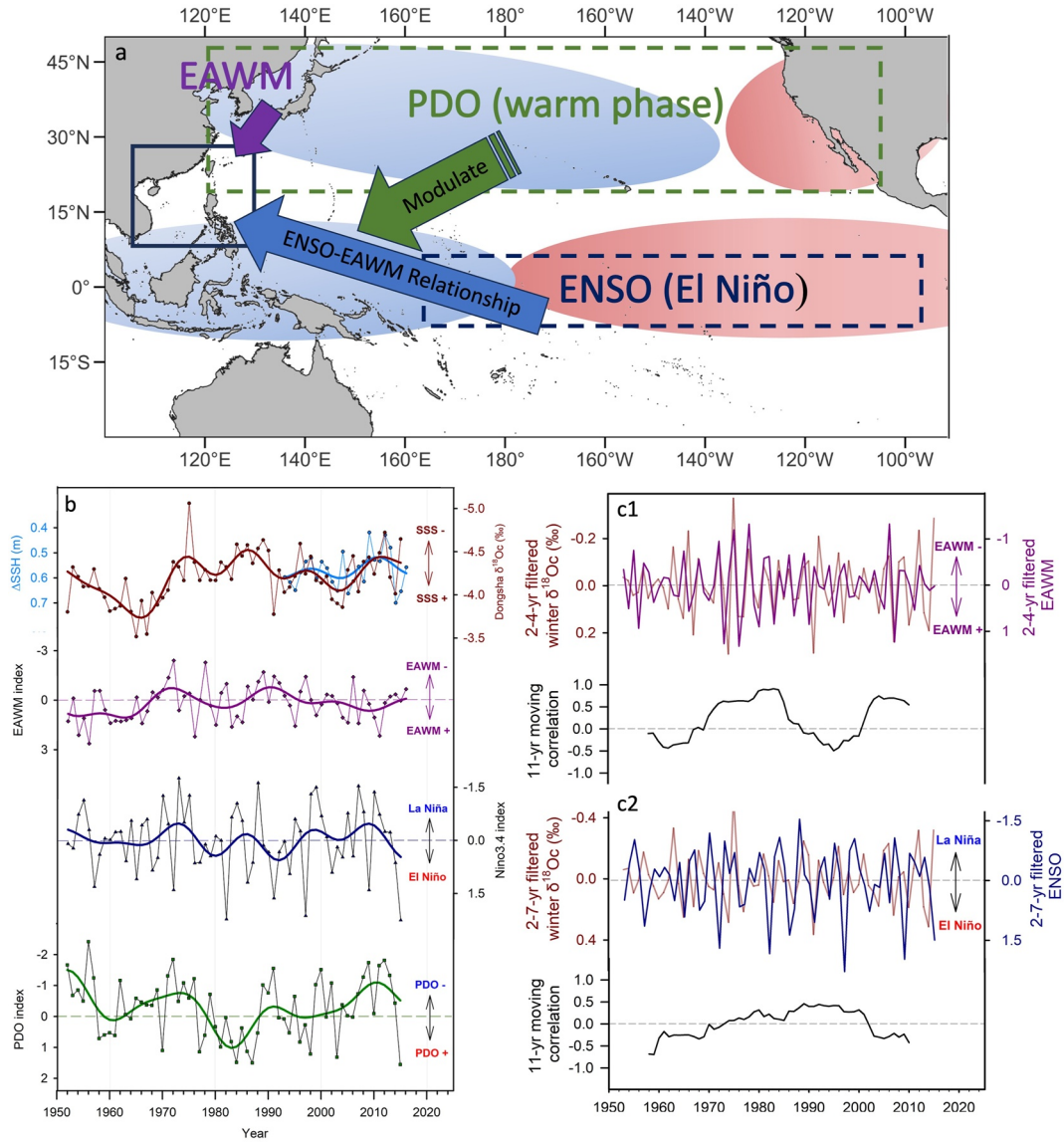

Figure 3. (a) Schematic of the driving forces, including the East Asian winter monsoon (EAWM), El Niño-Southern Oscillation (ENSO), and the Pacific Decadal Oscillation (PDO), that influence the Kuroshio intruding processes into the SCS. (b) The analysis of the annual dry season δ^{18}Oc values in Dongsha, comparing with several environmental indices: the ΔSSH record, the EAWM index, the Nino3.4 index, and the PDO index. The thin lines represent annual dry season change of the indices, while the thick lines show the index records after applying an 11-year low-pass filter. (c1) Upper: Comparison of the 2-4-year filtered records of Dongsha coral δ^{18}Oc and the EAWM index. Lower: 11-year moving correlation between the two records, which reveals a significant correlation from the 1970s to the 1980s, as well as the early 2000. (c2) Upper: Comparison of the 2-7-year filtered records of Dongsha coral δ^{18}Oc and the Nino3.4 index. Lower: 11-year moving correlation between the records, which shows a moderate-strong correlation between the 1980s and 1990s.

4.3. Dry-Season KI Variations and the Driving Forces

What may have caused the interannual to decadal changes in KI strength? Previous studies on geochemical signatures in corals from the SCS have linked the northern SCS climate variability on seasonal to decadal time scales to the activity of the East Asian monsoon, ENSO, and PDO (Figure 3a) (Deng et al., 2013; Han et al., 2020; X. Li et al., 2017, 2023; Ramos et al., 2020; Su et al., 2006; Yu et al., 2005). Very few of them however focus on KI variability, and typically in averaged the whole yearly signals are averaged for the comparisons (with a notable exception of Ramos et al. (2020)). Here, we used the winter-only indices of EAWM, Nino3.4, and PDO, averaged over the period from December to March of the following year (the dry season), to investigate the driving forces of the KI variations on interannual and decadal timescales (Figure 3).

The northern SCS is influenced by monsoons, particularly the EAWM, which plays an important role in ocean and climate variability on seasonal to interannual time scales (e.g., Jiang et al., 2023; Murty et al., 2017; Ramos et al., 2020). During weak EAWM periods, warmer and wetter conditions occur, leading to relatively low SSS in the SCS. When the intensity of the EAWM increases, a low-level northeasterly wind blowing from East Asia to the low latitudes in the western Pacific weakens the northward-flowing Kuroshio Current, resulting in enhanced KI with more salty water flowing into the SCS. To examine the influence of EAWM on surface water salinity in the northern SCS, we compared the dry season δ^{18}Oc values in Dongsha to the EAWM index (L. Wang & Chen, 2014). Because the spectral analysis shows interannual variability of δ^{18}Oc, we compared the 2-4-year filtered δ^{18}Oc and the EAWM index during the dry season (December–March) (Figure 3). The comparison reveals a robust correlation (i.e., correlation >0.6) during the 1970s and 1980s. The correlation was weaker during the 1990s and became enhanced again after the early 2000s. Similarly, cross-wavelet analysis conducted between Dongsha δ^{18}Oc and the EAWM index also reveals a noteworthy correlation in the 1970s–1980s and the early 2000s, within a period band of approximately 2–4 years (Figure S18 in Supporting Information S1).

ENSO plays a crucial role in impacting changes in SSS and the strength of the Kuroshio Current on interannual time scales (Weiss et al., 2021; C.-R. Wu, 2013). During El Niño years, the northward shift of the North Equatorial Current bifurcation latitude results in a weaker Kuroshio Current transport and stronger KI. Indeed, when comparing annual dry season Dongsha δ^{18}Oc with the ENSO index by Nino3.4 SST (https://climatedataguide.ucar.edu/climate-data/), we observed that elevated δ^{18}Oc values and increased KI strength tend to coincide with more positive Nino3.4 index values (Figure 3b). However, the correlation between the coral δ^{18}Oc and the ENSO index is rather weak and only reaches moderately strong between the 1980s and 1990s, as shown in their 2-7-year filtered data (Figure 3c). Consistently, cross-wavelet analysis only shows a relatively high correlation between the δ^{18}Oc and ENSO index in the 1980s–1990s, within a period band of approximately 4–6 years (Figure S18 in Supporting Information S1). On the decadal timescales, the cross-wavelet analysis indicates a strong correlation between the δ^{18}Oc and ENSO from the 1970s to the 1990s. However, the ENSO state remained neutral when the strongest KI occurred during the 1950s–1960s. It appears that ENSO and the EAWM may have alternatively dominated the influence on KI strength, particularly on the interannual timescales. For example, strong coherence between the EAWM and KI strength appears during the 1970s and 1980s as well as after the early 2000s, but strong coherence between ENSO and KI strength is observable during the 1980s and 1990s (Figure 3c; Figure S18 in Supporting Information S1).

The variability of the KI may not be solely attributed to the EAWM and ENSO. Our spectral analysis of Dongsha δ^{18}Oc reveals a distinct peak at a period of approximately 33 years (Figure S11 in Supporting Information S1), signifying decadal variability in the record with significance exceeding 90%. This decadal variability may appear to be influenced by the PDO. On the decadal timescale, statistical analysis has shown a strong connection between KI variables and the PDO phases from the 1990s to the 2010s (C.-R. Wu, 2013). The warm PDO phase during this period is linked to an anomalous anticyclonic wind field over the Philippine Sea, which reduces the Kuroshio Current transport off Luzon and increases the KI into the SCS. However, as depicted in Figure 3b; Figure S18 in Supporting Information S1, the correlation between the Dongsha δ^{18}Oc and the PDO remains weak during the 1950s and 1970s, when the PDO is in its cold phase. On the other hand, Dongsha δ^{18}Oc exhibits a negative association with the PDO during its warm phases in the 1980s (Figure 3b). This is in contrast to the view that KI strength would increase during the warm phase of the PDO (e.g., C.-R. Wu, 2013). When examining wavelet analyses, we did not observe robust signals at decadal timescales when comparing winter δ^{18}Oc to the PDO (Figure S18 in Supporting Information S1). This may result from the short duration of our record, so that the cone of influence in the wavelet analyses could not encompass specific segment for investigation. We suggest that the PDO may overall have a minor effect on KI strength. Alternatively, the PDO may indirectly modulate KI strength through its influence on ENSO activities. A warm PDO phase can enhance El Niño (J.-W. Kim et al., 2014; L. Wang et al., 2008), which can then intensify the water advection across the Luzon Strait into the SCS. Indeed, the most recent strong KI periods registered between 1990s and 2000s, when El Niño conditions dominated and the PDO was broadly in its warm phase (Figure 3b). Conversely, the cold PDO phase post the 2000s through 2010 probably favors La Niña conditions (J.-W. Kim et al., 2014; L. Wang et al., 2008), and they jointly weakened the KI. Nevertheless, longer records, particularly in situ observation data, are needed to further examine the interactions between the PDO and ENSO, and their impacts on KI strength.

5. Conclusions

In this study, we present a 60-year *Porites* δ^{18}Oc record from Dongsha Atoll, located in the northern SCS. Our results demonstrate that the coral δ^{18}O records can provide a reliable representation of the ocean surface

temperature and salinity conditions in the northern SCS. The SSS variation is highly influenced by the change in KI strength, as evidenced by the strong similarities between our δ^{18}Oc record and KI variability. We therefore used δ^{18}Oc to investigate regional hydrological changes. We found that the KI exhibits interannual to decadal-scale variabilities. Particularly on the interannual timescales, KI strength was predominantly controlled by the EAWM during the 1970s and 1980s and after the early 2000s, while KI strength was more influenced by ENSO between the 1980s and 1990s. Moreover, our study also highlights the PDO's indirect impacts on KI variability through its modulation on ENSO variations.

The KI plays a crucial role in shaping the hydrological conditions and marine ecosystem of the northern SCS. Its impacts on SST, SSS and nutrient availability can in turn have significant influences on the composition and distribution of regional marine communities. These alterations probably have cascading effects on trophic interactions, species dynamics, and biogeochemical processes in the marine environment. Climate models in general suggest that the EAWM will weaken in the future warming climate (e.g., Kang et al., 2022; Zhao et al., 2021). On the other hand, a majority of the models show a more frequent occurrence of El Niño events under anthropogenic warming (e.g., Cai et al., 2021). If the controlling mechanisms we identified hold true in the future, changes in EAWM and ENSO conditions will then have counteracting effects on KI's variability. Thus, it remains uncertain how future KI would impact the hydrological conditions and marine ecosystem in the northern SCS.

Conflict of Interest

The authors declare no conflicts of interest relevant to this study.

Data Availability Statement

The coral Sr/Ca, δ^{18}O, and ΔSSH data generated in this study are available in a Zenodo repository in Lin (2024).

Acknowledgments

We thank Dr. Ming-Shiou Jeng for his help in collecting the Dongsha coral core. Additionally, we extend our appreciation to Dr. Lim Ming Pin Alan and the Facility for Analysis, Characterization, Testing and Simulation (FACTS) laboratory at Nanyang Technological University for the support in conducting mineral diagenesis analysis. This work has been possible thanks to the support by the Earth Observatory of Singapore via its funding from the National Research Foundation Singapore (NRF) and the Singapore Ministry of Education (MOE) under the Research Centres of Excellence initiative. The study was also financially supported by the National Science and Technology Council (NSTC), Taiwan, under Grant NSTC111-2116-M-001-014 to Y.-G.C. T.H. acknowledges funding from the Natural Science Foundation of China (NSFC) under Grant 42103083, and from the China Postdoctoral Science Foundation under Grant 2021M693149. X.W. acknowledges the financial support from the Singapore Ministry of Education under Grant MOE-T2EP10122-0006. This work comprises Earth Observatory of Singapore contribution no. 566.

References

Adler, R. F., Huffman, G. J., Chang, A., Ferraro, R., Xie, P.-P., Janowiak, J., et al. (2003). The version-2 global precipitation climatology project (GPCP) monthly precipitation analysis (1979–present). *Journal of Hydrometeorology*, *4*(6), 1147–1167. https://doi.org/10.1175/1525-7541(2003)004<1147:tvgpcp>2.0.co;2

Alpert, A. E., Cohen, A. L., Oppo, D. W., DeCarlo, T. M., Gove, J. M., & Young, C. W. (2016). Comparison of equatorial Pacific sea surface temperature variability and trends with Sr/Ca records from multiple corals. *Paleoceanography*, *31*(2), 252–265. https://doi.org/10.1002/2015pa002897

Bolton, A., Goodkin, N. F., Hughen, K., Ostermann, D. R., Vo, S. T., & Phan, H. K. (2014). Paired Porites coral Sr/Ca and δ^{18}O from the western South China Sea: Proxy calibration of sea surface temperature and precipitation. *Palaeogeography, Palaeoclimatology, Palaeoecology*, *410*, 233–243. https://doi.org/10.1016/j.palaeo.2014.05.047

Cai, W., Santoso, A., Collins, M., Dewitte, B., Karamperidou, C., Kug, J.-S., et al. (2021). Changing El Niño–Southern Oscillation in a warming climate. *Nature Reviews Earth & Environment*, *2*(9), 628–644. https://doi.org/10.1038/s43017-021-00199-z

Caruso, M. J., Gawarkiewicz, G. G., & Beardsley, R. C. (2006). Interannual variability of the Kuroshio intrusion in the South China Sea. *Journal of Oceanography*, *62*(4), 559–575. https://doi.org/10.1007/s10872-006-0076-0

Centurioni, L. R., Niiler, P. P., & Lee, D.-K. (2004). Observations of inflow of Philippine Sea surface water into the South China Sea through the Luzon Strait. *Journal of Physical Oceanography*, *34*(1), 113–121. https://doi.org/10.1175/1520-0485(2004)034<0113:ooiops>2.0.co;2

Chang, Y., Shih, Y.-Y., Tsai, Y.-C., Lu, Y.-H., Liu, J. T., Hsu, T.-Y., et al. (2022). Decreasing trend of kuroshio intrusion and its effect on the chlorophyll-*a* concentration in the Luzon Strait, South China Sea. *GIScience & Remote Sensing*, *59*(1), 633–647. https://doi.org/10.1080/15481603.2022.2051384

Chen, C.-T. A. (2008). Distributions of nutrients in the East China Sea and the South China Sea connection. *Journal of Oceanography*, *64*(5), 737–751. https://doi.org/10.1007/s10872-008-0062-9

Chou, W., Sheu, D. D., Chen, C. T. A., Wen, L., Yang, Y., & Wei, C. (2007). Transport of the South China Sea subsurface water outflow and its influence on carbon chemistry of Kuroshio waters off southeastern Taiwan. *Journal of Geophysical Research*, *112*(C12), C12008. https://doi.org/10.1029/2007jc004087

Correge, T., Gagan, M. K., Beck, J. W., Burr, G. S., Cabioch, G., & Le Cornec, F. (2004). Interdecadal variation in the extent of South Pacific tropical waters during the Younger Dryas event. *Nature*, *428*(6986), 927–929. https://doi.org/10.1038/nature02506

Dassié, E. P., Linsley, B. K., Corrège, T., Wu, H. C., Lemley, G. M., Howe, S., & Cabioch, G. (2014). A Fiji multi-coral δ^{18}O composite approach to obtaining a more accurate reconstruction of the last two-centuries of the ocean-climate variability in the South Pacific Convergence Zone region. *Paleoceanography*, *29*(12), 1196–1213. https://doi.org/10.1002/2013pa002591

DeLong, K. L., Quinn, T. M., & Taylor, F. W. (2007). Reconstructing twentieth-century sea surface temperature variability in the southwest Pacific: A replication study using multiple coral Sr/Ca records from New Caledonia. *Paleoceanography*, *22*(4), PA4212. https://doi.org/10.1029/2007pa001444

Deng, W., Wei, G., Xie, L., Ke, T., Wang, Z., Zeng, T., & Liu, Y. (2013). Variations in the Pacific Decadal Oscillation since 1853 in a coral record from the northern South China Sea. *Journal of Geophysical Research: Oceans*, *118*(5), 2358–2366. https://doi.org/10.1002/jgrc.20180

Durack, P. J., Wijffels, S. E., & Matear, R. J. (2012). Ocean salinities reveal strong global water cycle intensification during 1950 to 2000. *Science*, *336*(6080), 455–458. https://doi.org/10.1126/science.1212222

Farris, A., & Wimbush, M. (1996). Wind-induced Kuroshio intrusion into the South China Sea. *Journal of Oceanography*, *52*(6), 771–784. https://doi.org/10.1007/bf02239465

Gagan, M. K., Chivas, A. R., & Isdale, P. J. (1994). High-resolution isotopic records from corals using ocean temperature and mass-spawning chronometers. *Earth and Planetary Science Letters*, *121*(3–4), 549–558. https://doi.org/10.1016/0012-821x(94)90090-6

Ghil, M., Allen, M. R., Dettinger, M. D., Ide, K., Kondrashov, D., Mann, M. E., et al. (2002). Advanced spectral methods for climatic time series. *Reviews of Geophysics*, *40*(1), 1–3. https://doi.org/10.1029/2000rg000092

Grinsted, A., Moore, J. C., & Jevrejeva, S. (2004). Application of the cross wavelet transform and wavelet coherence to geophysical time series. *Nonlinear Processes in Geophysics*, *11*(5/6), 561–566. https://doi.org/10.5194/npg-11-561-2004

Han, T., Yu, K., Yan, H., Jiang, W., Yan, H., & Tao, S. (2020). Coral δ^{18}O-based reconstruction of El Niño-Southern Oscillation from the northern South China Sea since 1851 AD. *Quaternary International*, *550*, 159–168. https://doi.org/10.1016/j.quaint.2020.04.032

He, X., Liu, D., Peng, Z., & Liu, W. (2002). Monthly sea surface temperature records reconstructed by δ^{18}O of reef-building coral in the east of Hainan Island, South China Sea. *Science in China, Series B: Chemistry*, *45*(S1), 130–136. https://doi.org/10.1007/bf02932214

Hu, J., Kawamura, H., Hong, H., & Qi, Y. (2000). A review on the currents in the South China Sea: Seasonal circulation, South China Sea warm current and Kuroshio intrusion. *Journal of Oceanography*, *56*(6), 607–624. https://doi.org/10.1023/a:1011117531252

Huang, B., Liu, C., Banzon, V., Freeman, E., Graham, G., Hankins, B., et al. (2021). Improvements of the daily optimum interpolation sea surface temperature (DOISST) version 2.1. *Journal of Climate*, *34*(8), 2923–2939. https://doi.org/10.1175/jcli-d-20-0166.1

Jiang, L., Yu, K., Tao, S., Jiang, W., Wang, S., & Li, Y. (2023). Modulation of East Asian monsoon strength by ENSO during the warm periods of the late Holocene: Evidence from Porites corals in the northern South China Sea. *Global and Planetary Change*, *225*, 104136. https://doi.org/10.1016/j.gloplacha.2023.104136

Kang, S., Wang, X., Du, J., & Song, Y. (2022). Paleoclimates inform on a weakening and amplitude-reduced East Asian winter monsoon in the warming future. *Geology*, *50*(11), 1224–1228. https://doi.org/10.1130/g50246.1

Kim, J.-W., Yeh, S.-W., & Chang, E.-C. (2014). Combined effect of El Niño-Southern Oscillation and Pacific Decadal Oscillation on the East Asian winter monsoon. *Climate Dynamics*, *42*(3–4), 957–971. https://doi.org/10.1007/s00382-013-1730-z

Kim, Y. Y., Qu, T., Jensen, T., Miyama, T., Mitsudera, H., Kang, H., & Ishida, A. (2004). Seasonal and interannual variations of the North Equatorial Current bifurcation in a high-resolution OGCM. *Journal of Geophysical Research*, *109*(C3), C03040. https://doi.org/10.1029/2003jc002013

Kuffner, I. B., Jokiel, P. L., Rodgers, K. S., Andersson, A. J., & Mackenzie, F. T. (2012). An apparent "vital effect" of calcification rate on the Sr/Ca temperature proxy in the reef coral *Montipora capitata*. *Geochemistry, Geophysics, Geosystems*, *13*(8), Q08004. https://doi.org/10.1029/2012gc004128

Lee, H.-J., Chao, S.-Y., Fan, K.-L., Wang, Y.-H., & Liang, N.-K. (1997). Tidally induced upwelling in a semi-enclosed basin: Nan Wan Bay. *Journal of Oceanography*, *53*, 467–480.

Li, G., Cheng, L., Pan, Y., Wang, G., Liu, H., Zhu, J., et al. (2023). A global gridded ocean salinity dataset with 0.5° horizontal resolution since 1960 for the upper 2000 m. *Frontiers in Marine Science*, *10*, 446. https://doi.org/10.3389/fmars.2023.1108919

Li, T., Zhao, J., Sun, R., Chang, F., & Sun, H. (2010). The variation of upper ocean structure and paleoproductivity in the Kuroshio source region during the last 200 Kyr. *Marine Micropaleontology*, *75*(1–4), 50–61. https://doi.org/10.1016/j.marmicro.2010.02.005

Li, X., Liu, Y., Hsin, Y., Liu, W., Shi, Z., Chiang, H., & Shen, C. (2017). Coral record of variability in the upstream Kuroshio Current during 1953–2004. *Journal of Geophysical Research: Oceans*, *122*(8), 6936–6946. https://doi.org/10.1002/2017jc012944

Li, X., Ma, J., Liu, Y., Hu, S., Sun, W., Nan, F., & Shen, C.-C. (2023). A monthly resolved coral δ^{13}C and δ^{18}O record of changes in the Kuroshio Current into the South China Sea via the Luzon Strait. *Palaeogeography, Palaeoclimatology, Palaeoecology*, *615*, 111468. https://doi.org/10.1016/j.palaeo.2023.111468

Liang, W., Yang, Y. J., Tang, T. Y., & Chuang, W. (2008). Kuroshio in the Luzon Strait. *Journal of Geophysical Research*, *113*(C8), C08048. https://doi.org/10.1029/2007jc004609

Lin, K. (2024). The coral Sr/Ca, δ^{18}O and ΔSSH data for article "influences of East Asian winter monsoon and El Niño-Southern Oscillation variability on the Kuroshio intrusion to the South China Sea over the past 60 years" [Dataset]. Zenodo. https://doi.org/10.5281/zenodo.10459147

Linsley, B. K., Wellington, G. M., Schrag, D. P., Ren, L., Salinger, M. J., & Tudhope, A. W. (2004). Geochemical evidence from corals for changes in the amplitude and spatial pattern of South Pacific interdecadal climate variability over the last 300 years. *Climate Dynamics*, *22*, 1–11. https://doi.org/10.1007/s00382-003-0364-y

Liu, T., Schmitt, R. W., & Li, L. (2018). Global search for autumn-lead sea surface salinity predictors of winter precipitation in southwestern United States. *Geophysical Research Letters*, *45*(16), 8445–8454. https://doi.org/10.1029/2018gl079293

Liu, T., Xu, J., He, Y., Lü, H., Yao, Y., & Cai, S. (2016). Numerical simulation of the Kuroshio intrusion into the South China Sea by a passive tracer. *Acta Oceanologica Sinica*, *35*(9), 1–12. https://doi.org/10.1007/s13131-016-0930-x

Lough, J. M. (2010). Climate records from corals. *Wiley Interdisciplinary Reviews: Climate Change*, *1*(3), 318–331. https://doi.org/10.1002/wcc.39

Marshall, J. F., & McCulloch, M. T. (2002). An assessment of the Sr/Ca ratio in shallow water hermatypic corals as a proxy for sea surface temperature. *Geochimica et Cosmochimica Acta*, *66*(18), 3263–3280. https://doi.org/10.1016/s0016-7037(02)00926-2

McConnaughey, T. (1989). ^{13}C and ^{18}O isotopic disequilibrium in biological carbonates: I. Patterns. *Geochimica et Cosmochimica Acta*, *53*(1), 151–162. https://doi.org/10.1016/0016-7037(89)90282-2

Murty, S. A., Bernstein, W. N., Ossolinski, J. E., Davis, R. S., Goodkin, N. F., & Hughen, K. A. (2018). Spatial and temporal robustness of Sr/Ca-SST calibrations in Red Sea corals: Evidence for influence of mean annual temperature on calibration slopes. *Paleoceanography and Paleoclimatology*, *33*(5), 443–456. https://doi.org/10.1029/2017pa003276

Murty, S. A., Goodkin, N. F., Halide, H., Natawidjaja, D., Suwargadi, B., Suprihanto, I., et al. (2017). Climatic influences on southern Makassar Strait salinity over the past century. *Geophysical Research Letters*, *44*(23), 11–967. https://doi.org/10.1002/2017gl075504

Nan, F., Xue, H., Chai, F., Shi, L., Shi, M., & Guo, P. (2011). Identification of different types of Kuroshio intrusion into the South China Sea. *Ocean Dynamics*, *61*(9), 1291–1304. https://doi.org/10.1007/s10236-011-0426-3

Nan, F., Xue, H., Chai, F., Wang, D., Yu, F., Shi, M., et al. (2013). Weakening of the Kuroshio intrusion into the South China Sea over the past two decades. *Journal of Climate*, *26*(20), 8097–8110. https://doi.org/10.1175/jcli-d-12-00315.1

Nan, F., Xue, H., & Yu, F. (2015). Kuroshio intrusion into the South China Sea: A review. *Progress in Oceanography*, *137*, 314–333. https://doi.org/10.1016/j.pocean.2014.05.012

Nurhati, I. S., Cobb, K. M., & Di Lorenzo, E. (2011). Decadal-scale SST and salinity variations in the central tropical Pacific: Signatures of natural and anthropogenic climate change. *Journal of Climate*, *24*(13), 3294–3308. https://doi.org/10.1175/2011jcli3852.1

Qu, T., Kim, Y. Y., Yaremchuk, M., Tozuka, T., Ishida, A., & Yamagata, T. (2004). Can Luzon Strait transport play a role in conveying the impact of ENSO to the South China Sea? *Journal of Climate*, *17*(18), 3644–3657. https://doi.org/10.1175/1520-0442(2004)017<3644:clstpa>2.0.co;2

Quinn, T. M., & Sampson, D. E. (2002). A multiproxy approach to reconstructing sea surface conditions using coral skeleton geochemistry. *Paleoceanography*, *17*(4), 11–14. https://doi.org/10.1029/2000pa000528

Ramos, R. D., Goodkin, N. F., & Fan, T. (2020). Coral records at the northern edge of the Western Pacific Warm Pool reveal multiple drivers of sea surface temperature, salinity, and rainfall variability since the end of the Little Ice Age. *Paleoceanography and Paleoclimatology*, *35*(5), e2019PA003826. https://doi.org/10.1029/2019pa003826

Rong, Z., Liu, Y., Zong, H., & Cheng, Y. (2007). Interannual sea level variability in the South China Sea and its response to ENSO. *Global and Planetary Change*, *55*(4), 257–272. https://doi.org/10.1016/j.gloplacha.2006.08.001

Sayani, H. R., Cobb, K. M., DeLong, K., Hitt, N. T., & Druffel, E. R. M. (2019). Intercolony $\delta^{18}O$ and Sr/Ca variability among Porites spp. corals at Palmyra Atoll: Toward more robust coral-based estimates of climate. *Geochemistry, Geophysics, Geosystems*, *20*(11), 5270–5284. https://doi.org/10.1029/2019gc008420

SChmitt, R. W. (2008). Salinity and the global water cycle. *Oceanography*, *21*(1), 12–19. https://doi.org/10.5670/oceanog.2008.63

Shaw, P. (1991). The seasonal variation of the intrusion of the Philippine Sea water into the South China Sea. *Journal of Geophysical Research*, *96*(C1), 821–827. https://doi.org/10.1029/90jc02367

Shen, C.-C., Lee, T., Chen, C.-Y., Wang, C.-H., Dai, C.-F., & Li, L.-A. (1996). The calibration of D [Sr/Ca] versus sea surface temperature relationship for Porites corals. *Geochimica et Cosmochimica Acta*, *60*(20), 3849–3858. https://doi.org/10.1016/0016-7037(96)00205-0

Shen, C.-C., Liu, K.-K., Lee, M.-Y., Lee, T., Wang, C.-H., & Lee, H.-J. (2005). A novel method for tracing coastal water masses using Sr/Ca ratios and salinity in Nanwan Bay, southern Taiwan. *Estuarine, Coastal and Shelf Science*, *65*(1–2), 135–142. https://doi.org/10.1016/j.ecss.2005.05.010

Shen, X., Hu, B., Yan, H., Dodson, J., Zhao, J., Li, J., et al. (2022). Reconstruction of Kuroshio intrusion into the South China Sea over the last 40 Kyr. *Quaternary Science Reviews*, *290*, 107622. https://doi.org/10.1016/j.quascirev.2022.107622

Shu, Y., Wang, Q., & Zu, T. (2018). Progress on shelf and slope circulation in the northern South China Sea. *Science China Earth Sciences*, *61*(5), 560–571. https://doi.org/10.1007/s11430-017-9152-y

Su, R., Sun, D., Bloemendal, J., & Zhu, Z. (2006). Temporal and spatial variability of the oxygen isotopic composition of massive corals from the South China Sea: Influence of the Asian monsoon. *Palaeogeography, Palaeoclimatology, Palaeoecology*, *240*(3–4), 630–648. https://doi.org/10.1016/j.palaeo.2006.03.012

Terray, L., Corre, L., Cravatte, S., Delcroix, T., Reverdin, G., & Ribes, A. (2012). Near-surface salinity as nature's rain gauge to detect human influence on the tropical water cycle. *Journal of Climate*, *25*(3), 958–977. https://doi.org/10.1175/jcli-d-10-05025.1

Wang, B., Wu, R., & Fu, X. (2000). Pacific–East Asian teleconnection: How does ENSO affect East Asian climate? *Journal of Climate*, *13*(9), 1517–1536. https://doi.org/10.1175/1520-0442(2000)013<1517:peathd>2.0.co;2

Wang, L., & Chen, W. (2014). An intensity index for the East Asian winter monsoon. *Journal of Climate*, *27*(6), 2361A–2374.

Wang, L., Chen, W., & Huang, R. (2008). Interdecadal modulation of PDO on the impact of ENSO on the East Asian winter monsoon. *Geophysical Research Letters*, *35*(20), L20702. https://doi.org/10.1029/2008gl035287

Wang, Y., Yu, Y., Zhang, Y., Zhang, H.-R., & Chai, F. (2020). Distribution and variability of sea surface temperature fronts in the South China Sea. *Estuarine, Coastal and Shelf Science*, *240*, 106793. https://doi.org/10.1016/j.ecss.2020.106793

Watanabe, T., Juillet-Leclerc, A., Cuif, J.-P., Rollion-Bard, C., Dauphin, Y., & Reynaud, S. (2007). Recent advances in coral biomineralization with implications for paleo-climatology: A brief overview. In *Elsevier oceanography series* (Vol. 73, pp. 239–495).

Weiss, T. L., Linsley, B. K., & Gordon, A. L. (2021). Pacific North Equatorial Current bifurcation latitude and Kuroshio Current shifts since the Last Glacial Maximum inferred from a Sulu Sea thermocline reconstruction. *Quaternary Science Reviews*, *264*, 106999. https://doi.org/10.1016/j.quascirev.2021.106999

Wu, C., & Hsin, Y. (2012). The forcing mechanism leading to the Kuroshio intrusion into the South China Sea. *Journal of Geophysical Research*, *117*(C7), C07015. https://doi.org/10.1029/2012jc007968

Wu, C.-R. (2013). Interannual modulation of the Pacific Decadal Oscillation (PDO) on the low-latitude western North Pacific. *Progress in Oceanography*, *110*, 49–58. https://doi.org/10.1016/j.pocean.2012.12.001

Wu, C.-R., Wang, Y.-L., Lin, Y.-F., & Chao, S.-Y. (2017). Intrusion of the Kuroshio into the south and East China Seas. *Scientific Reports*, *7*(1), 1–8. https://doi.org/10.1038/s41598-017-08206-4

Xu, C., Pumijumnong, N., Nakatsuka, T., Sano, M., & Li, Z. (2015). A tree-ring cellulose $\delta^{18}O$-based July–October precipitation reconstruction since AD 1828, northwest Thailand. *Journal of Hydrology*, *529*, 433–441. https://doi.org/10.1016/j.jhydrol.2015.02.037

Xu, F.-H., & Oey, L.-Y. (2015). Seasonal SSH variability of the northern South China Sea. *Journal of Physical Oceanography*, *45*(6), 1595–1609. https://doi.org/10.1175/jpo-d-14-0193.1

Xue, H., Chai, F., Pettigrew, N., Xu, D., Shi, M., & Xu, J. (2004). Kuroshio intrusion and the circulation in the South China Sea. *Journal of Geophysical Research*, *109*(C2), C02017. https://doi.org/10.1029/2002jc001724

Yu, K.-F., Zhao, J.-X., Wei, G.-J., Cheng, X.-R., Chen, T.-G., Felis, T., et al. (2005). $\delta^{18}O$, Sr/Ca and Mg/Ca records of Porites lutea corals from Leizhou Peninsula, northern South China Sea, and their applicability as paleoclimatic indicators. *Palaeogeography, Palaeoclimatology, Palaeoecology*, *218*(1–2), 57–73. https://doi.org/10.1016/j.palaeo.2004.12.003

Yuan, Y., Liao, G., Yang, C., Liu, Z., Chen, H., & Wang, Z.-G. (2014). Summer Kuroshio intrusion through the Luzon Strait confirmed from observations and a diagnostic model in summer 2009. *Progress in Oceanography*, *121*, 44–59. https://doi.org/10.1016/j.pocean.2013.10.003

Zhao, S., Feng, T., Tie, X., Li, G., & Cao, J. (2021). Air pollution zone migrates south driven by East Asian winter monsoon and climate change. *Geophysical Research Letters*, *48*(10), e2021GL092672. https://doi.org/10.1029/2021gl092672